

Tectonic and climate control of oil shale deposition in the Upper Cretaceous Qingshankou Formation (Songliao Basin, NE China)

Jianliang Jia · Zhaojun Liu · Achim Bechtel ·
Susanne A. I. Strobl · Pingchang Sun

Received: 29 November 2011 / Accepted: 21 April 2013 / Published online: 16 May 2013
© Springer-Verlag Berlin Heidelberg 2013

Abstract Oil shales were deposited in the Songliao Basin (NE China) during the Upper Cretaceous period, representing excellent hydrocarbon source rocks. High organic matter (OM) contents, a predominance of type-I kerogen, and a low maturity of OM in the oil shales are indicated by bulk geochemical parameters and biomarker data. A major contribution of aquatic organisms and minor inputs from terrigenous land plants to OM input are indicated by *n*-alkane distribution patterns, composition of steroids, and organic macerals. Strongly reducing bottom water conditions during the deposition of the oil shale sequences are indicated by low pristane/phytane ratios, high C_{14} -aryl-isoprenoid contents, homohopane distribution patterns, and high V/Ni ratios. Enhanced salinity stratification with mesosaline and alkaline bottom waters during deposition of the oil shales are

indicated by high gammacerane index values, low MTTC ratios, high β -carotene contents, low TOC/S ratios, and high Sr/Ba ratios. The stratified water column with anoxic conditions in the bottom water enhanced preservation of OM. Moderate input of detrital minerals during the deposition of the oil shale sequences is reflected by titanium concentrations. In this study, environmental conditions in the paleo-lake leading to OM accumulation in the sediments are related to sequence stratigraphy governed by climate and tectonics. The first Member of the Qingshankou Formation (K_2qn_1) in the Songliao Basin, containing the oil shale sequence, encompasses a third-order sequence that can be divided into three system tracts (transgressive system tract—TST, highstand system tract—HST, and regressive system tract—RST). Enrichment of OM changed from low values during TST-I to high-moderate values during TST-II/III and HST-I/II. Low OM enrichment occurs during RST-I and RST-II. Therefore, the highest enrichment of OM in the sediments is related to stages of mid-late TST and early HST.

J. Jia (✉)
Institute of Geology, Chinese Academy of Geological Sciences,
Beijing 100037, China
e-mail: jlja82@yahoo.cn

J. Jia · Z. Liu · P. Sun
College of Earth Sciences, Jilin University,
Changchun 130061, China

Z. Liu
e-mail: liuzj@jlu.edu.cn

P. Sun
e-mail: sunpingchang711@126.com

J. Jia · A. Bechtel · S. A. I. Strobl
Department Applied Geosciences and Geophysics,
Montanuniversität Leoben, Peter-Tunner-Str. 5,
8700 Leoben, Austria

A. Bechtel
e-mail: Achim.Bechteler@mu-leoben.at

S. A. I. Strobl
e-mail: Susanne.Strobl@unileoben.ac.at

Keywords Songliao Basin · Oil shale · Biomarker ·
Paleo-lake environment · Climate and tectonics

Introduction

Oil shales with high organic carbon contents are often considered to be excellent hydrocarbon source rocks (Feng et al. 2009a). The Songliao Basin in north-eastern China, with an area of approximately 26×10^4 km², contains over 10 km of Cretaceous sediments (Gao and Cai 1997). The basin has attracted considerable attention in recent years because of the huge potential of oil shale resource (Liu and Liu 2005; He et al. 2006; Qu et al. 2006; Wang 2006; Feng et al. 2009a; Liu et al. 2009, 2010; Chi 2010; Jia et al.

2011, 2012; Bechtel et al. 2012). However, detailed insights into the enrichment of the organic matter during the deposition of the oil shale-bearing formations are lacking. Such information is required to establish the relationship between changing environmental conditions of oil shale formation and lake-level fluctuations, climate change, and sequence stratigraphy (Bechtel et al. 2012).

The development of lacustrine hydrocarbon source rocks is controlled by basin morphology and depositional environment (Carroll and Bohacs 1999, 2001; Bohacs et al. 2000; Feng et al. 2011; Jia et al. 2013). The production and accumulation of OM are strongly influenced by the lake type (Bohacs et al. 2000), controlled by tectonics and climate (Carroll and Bohacs 1999). The oil shales of the Songliao Basin developed during a period of warm-humid climate and tectonic subsidence (Feng et al. 2010; Wang et al. 2012). The formation and evolution of the basin have been extensively studied (Liu et al. 1993; Wang et al. 1996; Feng et al. 2010). During the post-rift thermal subsidence period of the basin's evolution, eutrophic and anoxic conditions were established in the deep freshwater lake (Bechtel et al. 2012).

The molecular composition of OM provides information on the thermal history of sedimentary basins, the type and origin of OM, and environmental conditions, including water salinity and climate (Tissot and Welte 1984; Peters et al. 2005). As with many other non-marine, organic-rich petroleum source rocks in China, the deposition of oil shales may be associated with marine transgressions or saline lakes (Bechtel et al. 2012). Previous palaeontological and biomarker studies have provided geochemical evidence for marine transgressional events during the deposition of the oil shale sequences in the Qingshankou Formation of the Songliao Basin (Hou et al. 2000; Feng et al. 2009a). However, the molecular and isotopic compositions indicate a predominantly aquatic organic input to the oil shales (Feng et al. 2007). The presence of specific biomarkers in the oil shales within the K_2qn_1 of the Songliao Basin indicates a lagoonal depositional environment characterized by water stratification and high salinity (Feng et al. 2011; Bechtel et al. 2012).

In this study, based on sampled core profiles from the Qingshankou Formation of the Songliao Basin, we relate changes in the OM input and sedimentary environment during the deposition of the oil shale sequences to sequence stratigraphy.

Geological setting

The Songliao Basin, located in the north-east of China, is the largest oil- and gas-prone non-marine basin in China and can be divided into six primary tectonic units: the

northern plunge zone, the central downwarp zone, the north-eastern uplift zone, the south-eastern uplift zone, the south-western uplift zone, and the western slope zone (Feng et al. 2010) (Fig. 1). Oil shales are distributed mainly in the south-eastern uplift zone, the north-eastern uplift zone, and the central downwarp zone. The sediments of the basin are dominated by Cretaceous terrigenous successions. The Upper Cretaceous strata consist from bottom to top of the Qingshankou (K_2qn), the Yaojia (K_2y), the Nenjiang (K_2n), the Sifangtai (K_2s), and the Mingshui (K_2m) Formations (Fig. 2). Oil shales are mainly concentrated in the Qingshankou (K_2qn) and the Nenjiang (K_2n) Formations.

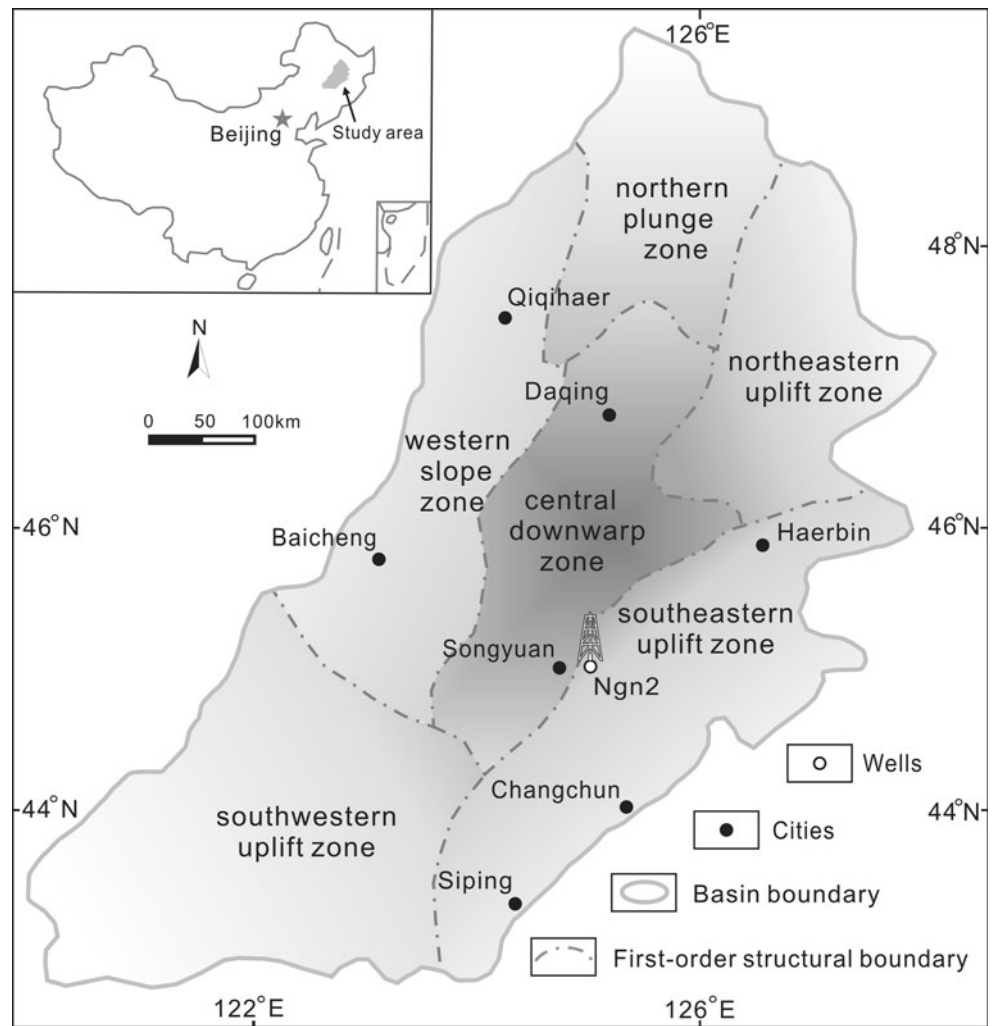
The basin was formed and filled in four tectonic evolutionary stages: a pre-rift doming stage, a syn-rift subsidence stage (fault subsidence), a post-rift thermal subsidence stage (depression), and a structural inversion stage (shrinkage) (Feng et al. 2010; Wang et al. 2012) (Fig. 2). During the Cretaceous period, a humid to semi-humid and subtropical climate prevailed (Huang et al. 1999a; Wang et al. 2012). In the Songliao Basin, the four cooling events (K_1h – K_1sh , K_1d_4 , K_2n , and K_2m_2), three warming events (K_1d_1 – K_1d_2 , K_2qn – K_2y , and K_2s), and three semi-arid events (K_1sh_3 – K_1sh_4 , K_1d_4 , and K_2s) (Fig. 2) are confirmed by evidence from spore/pollen and plant fossils, oxygen isotope data, and palaeoecology (Wang et al. 2012).

A cyclic evolution of the sedimentary basin has been outlined, controlled by tectonic and climatic changes (Fig. 2). During the deposition of the early Qingshankou and the early Nenjiang Formations, two transgression events (Liu et al. 1993) associated with basin subsidence and warm-humid climate led to the maximum depth and extent of the paleo-lake, covering an area of 8.7×10^4 and 20×10^4 km², respectively (Feng et al. 2010). The warm and humid climate during these stages of basin evolution promoted blooms of aquatic organisms, and the stable water column stratification was beneficial for organic matter preservation, resulting in the deposition of oil shales.

Samples and method

The samples were taken from Well Ngn2, which was drilled in 2007 and is located in the basin's south-east uplift zone (Fig. 1). The depth of the fully cored Well Ngn2 is 331 m, comprising the Quantou and the Qingshankou Formations (Fig. 3). We selected 64 samples (oil shale and mudstone) from the first Member of the Qingshankou Formation (K_2qn_1) for elemental (C, S) and Rock-Eval analyses (Fig. 3). Based on these results, 23 samples were selected for detailed biomarker and trace element measurements (Fig. 3).

Fig. 1 Zoning map of structural units of the Songliao Basin (modified according to Feng et al. 2010)



The total carbon (TC) and sulphur (S) contents were determined with a Leco elemental analyser. Total organic carbon (TOC) was measured with the same instrument on samples pre-treated with concentrated HCl. Pyrolysis was carried out using a Delsi Rock-Eval Version RE II instrument. With this method, the quantity of pyrolyzate (mg HC/g rock) generated from the kerogen during gradual heating in a helium stream is normalized to TOC to give the hydrogen index (HI, mg HC/g TOC). The temperature of maximum generation (T_{\max}) serves as a maturation indicator.

For organic geochemical analyses, representative portions of selected sediment samples were extracted for approximately 1 h using CH_2Cl_2 in a Dionex ASE 200 accelerated solvent extractor at 75 °C and 5×10^6 Pa. After evaporation of the solvent to 1 ml total solution in a Zymark TurboVap 500 closed cell concentrator, asphaltene were precipitated from a hexane- CH_2Cl_2 solution (80:1) and separated by centrifugation. The fractions of the hexane-soluble OM were separated into polar compounds, saturated hydrocarbons, and aromatic hydrocarbons by

medium-pressure liquid chromatography using a Köhnen-Willsch MPLC instrument (Radke et al. 1980).

The saturated and aromatic hydrocarbon fractions were analysed on a gas chromatograph equipped with a 30 m DB-5MS fused silica capillary column (i.d. 0.25 mm; 0.25 μm film thickness) and coupled to a Finnigan MAT GCQ ion trap mass spectrometer. The oven temperature was programmed from 70 to 300 °C at a rate of 4 °C min^{-1} , followed by an isothermal period of 15 min. Helium was used as carrier gas. The sample was not split and was injected at 275 °C. The mass spectrometer was operated in the EI (electron impact) mode over a scan range from m/z 50 to m/z 650 (0.7 s total scan time). Data were processed with a Finnigan data system. Identification of individual compounds was accomplished based on retention time in the total ion current (TIC) chromatogram and comparison of the mass spectra with published data. Relative percentages of different compound groups in the saturated and aromatic hydrocarbon fractions were calculated using peak areas from the gas chromatograms in relation to those of internal standards (deuterated *n*-tetracosane and 1,1'-binaphthyl, respectively).

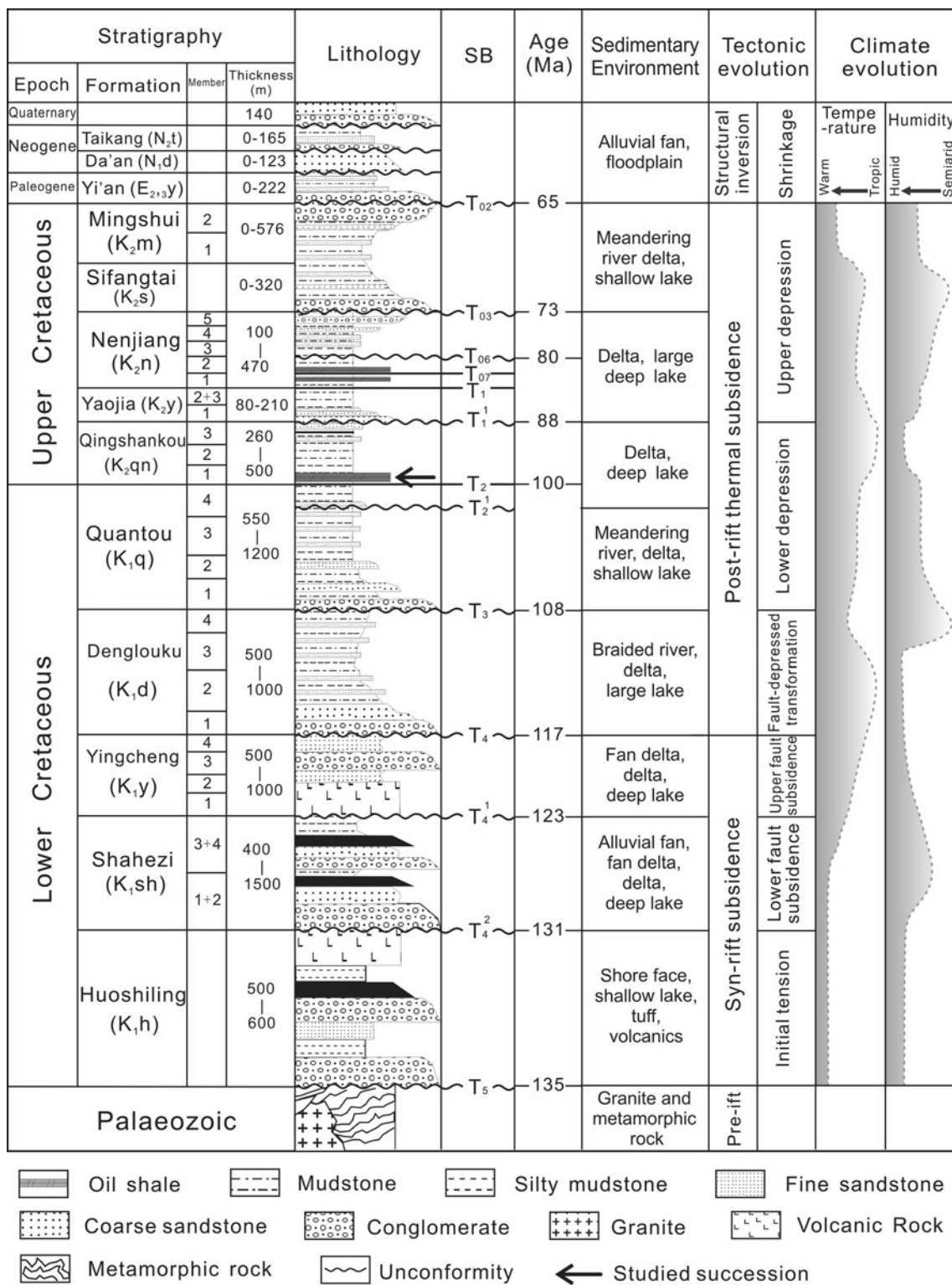
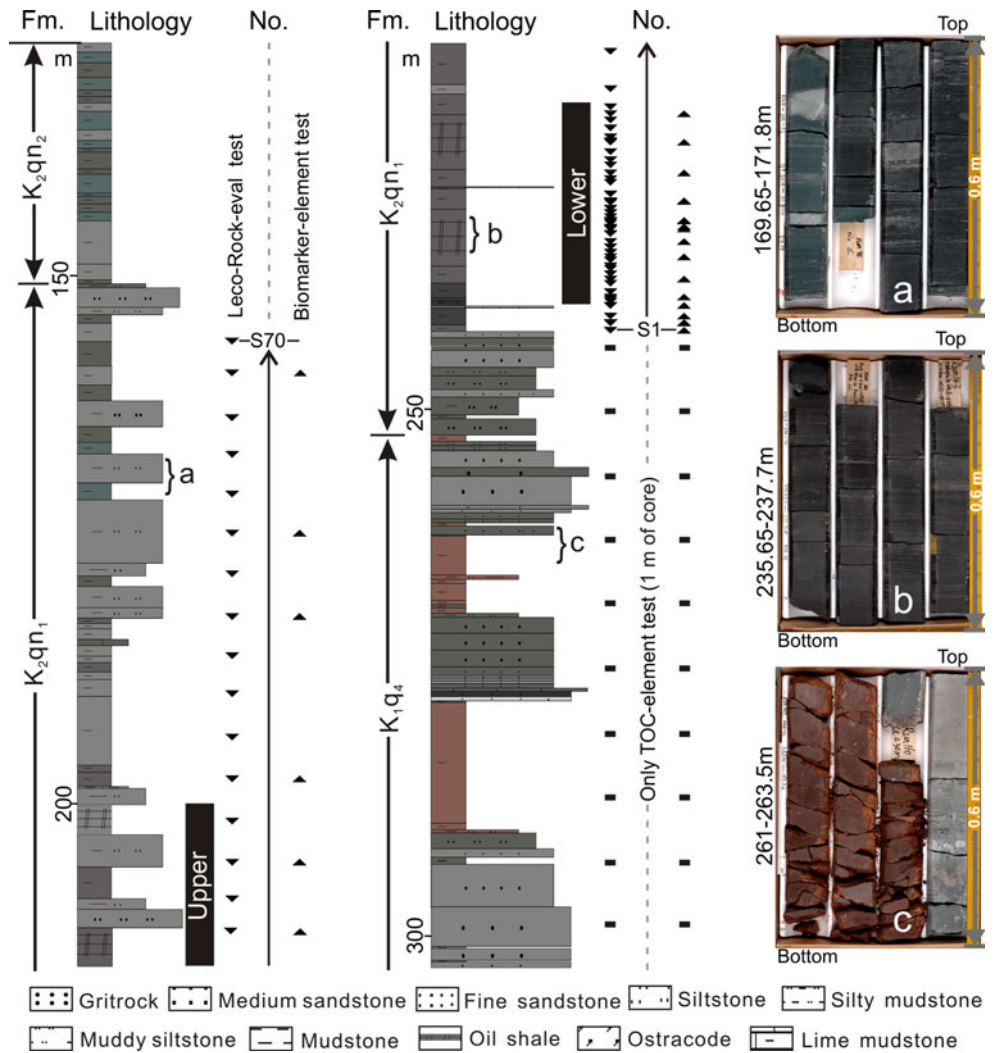


Fig. 2 Integrated interpretation of stratigraphic column of the Songliao Basin [modified according to Liu et al. (2002), Feng et al. (2010), Wang et al. (2012)]. SB sequence boundary

All samples were analysed for elements using a high-resolution inductively coupled plasma mass spectrometer (HR-ICP-MS) at the Analytical Laboratory of the

Beijing Research Institute of Uranium Geology. The samples for element analysis were all crushed and ground to <200 mesh. The analytical precision is

Fig. 3 Lithologic profile with position of test samples and photographs of cores from Well Ngn2. *Fm.* formation, *No.* number



estimated to be <5 % according to duplicate analysis of samples and standards.

Results and discussion

Bulk and Rock-Eval parameters

TOC content is an important indicator for OM abundance (Tissot and Welte 1984; Peters 1986). The TOC content of the oil shale within the first Member of the Qingshankou Formation (K₂qn₁) varies between 5.13 and 23.82 wt%, exceeding the average TOC obtained from the mudstone samples (3.16 wt%) (Fig. 4a). The total sulphur (S) content of the oil shales is highly variable (0.98–5.29 wt%), and a high average sulphur content is obtained within the K₂qn₁ (2.0 wt%). Most mudstones show lower sulphur content (avg. 1.62 wt%) (Fig. 4b).

The potential yield (S1 + S2) is a measure for the hydrocarbon generation potential of rocks. The S2

contents predominate over the S1 contents by far in all sediments of the K₂qn₁ (Fig. 4c), indicating the dominant role of pyrolytic hydrocarbons. The potential yield of the oil shale varies between 34.66 and 179.66 mg HC/g rock, higher than the values obtained from the mudstones (avg. 19.06 mg HC/g rock) (Fig. 4d). The highest hydrogen index (HI) values above 600 mg HC/g TOC are obtained from the oil shale sequences (Fig. 4e), and the low *T*_{max} values (430–440 °C) indicate marginal maturity of the oil shales around 0.5 % vitrinite reflectance values (Vr) (Bechtel et al. 2012). The trend in *T*_{max} towards slightly lower values with depth may be caused by a change in kerogen-type towards pure Type-I of the oil shale sequences. In the HI versus *T*_{max} diagram (Espitalié et al. 1984; Fig. 5), most oil shale samples fall inside the field characteristic for Type-I kerogen, except for a few in the Type-II area, indicating aquatic organisms as the main primary producers of OM. Minor admixture of Type-III kerogen (terrigenous OM) or mineral matrix effects of a few mudstone samples may cause deviation towards lower

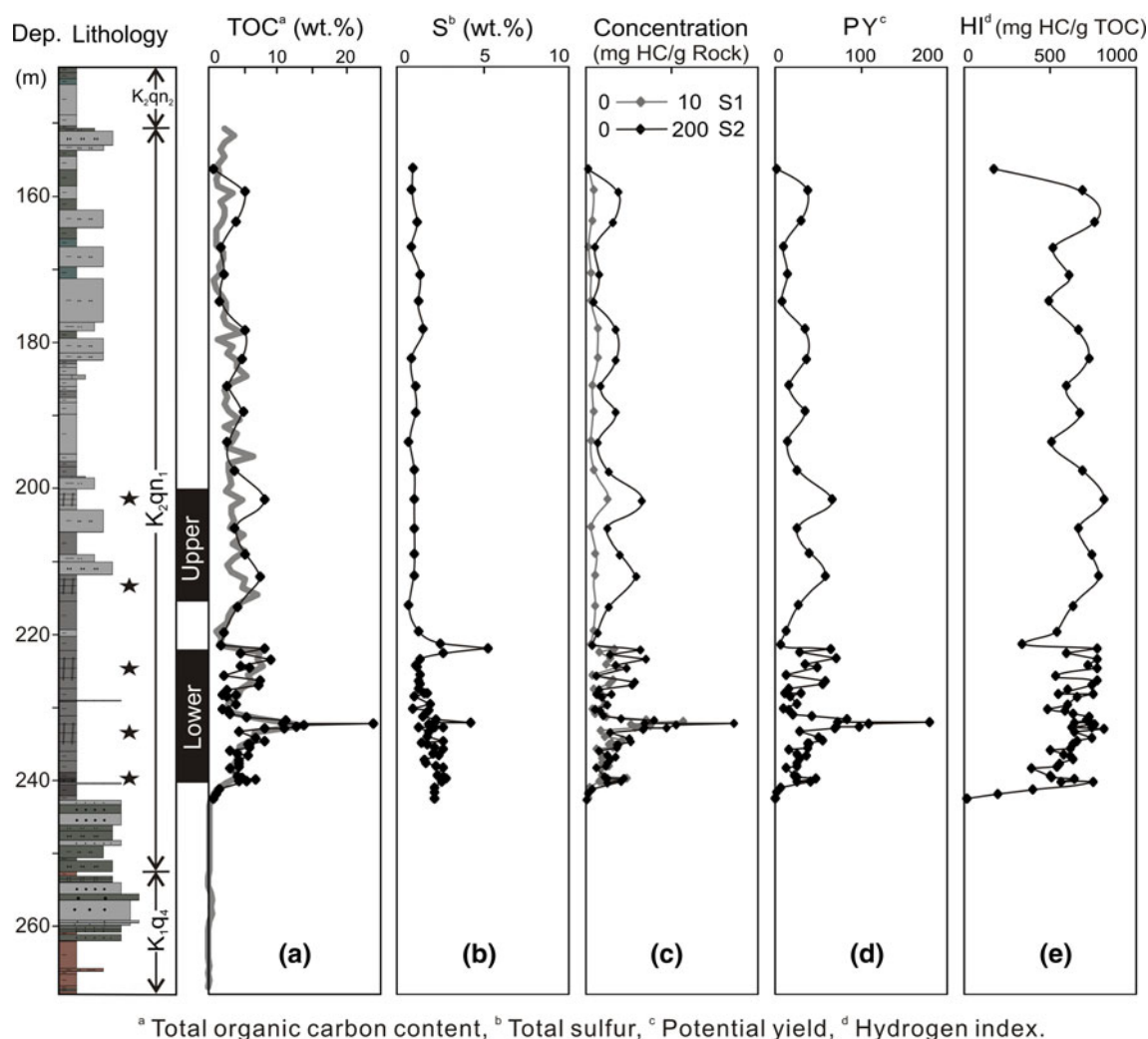


Fig. 4 Bulk organic geochemical parameters of Well Ngn2 in the Qingshankou Formation. The grey line in the TOC depth trend represents average TOC content of 1 m of core. Dep. depth

HI values. The HI versus oxygen index (OI) diagram has not been applied because of unreliable OI values.

Molecular composition of saturated and aromatic hydrocarbon fractions

The quantities of chloroform bitumen “A” in the kerogen of the oil shale samples in the K₂qn₁ vary between 0.12 and 1.02 wt%, with an average value of 0.45 wt%, exceeding by far the values obtained from mudstones (avg. 0.11 wt%) (Table 1). The data argue for abundant lipid-rich OM input during the deposition of the oil shale sequences.

Oil shales of K₂qn₁ are characterized by high quantities of *n*-alkanes (474–1,619 μg/g TOC) (Table 1; Fig. 6a). In the mass chromatograms of the saturated hydrocarbon fractions, abundant hopanoids (C_{29–30}) (250–1,239 μg/g TOC) (Table 1; Fig. 6b), gammacerane (Fig. 6a), and low quantities of β-carotene (21.4–66.2 μg/g TOC) (Table 1;

Fig. 6a) are present. Moreover, abundant steranes (C_{27–29}) (823 μg/g TOC) (Table 1; Fig. 6c), and highly variable contents of 4-methylsteranes (C_{28–30}) (948 μg/g TOC) (Table 1; Fig. 6d) are detected. In the mass chromatograms of aromatic hydrocarbon fractions, a series of monoaromatic steroids, benzohopanes aryl-isoprenoids, and methylated 2-methyl-2-(trimethyltridecyl) chromans (MTTCs) occur (Table 1).

The molecular composition of the hydrocarbons within the Qingshankou Formation has recently been described in detail by Bechtel et al. (2012). For the sequence stratigraphic interpretation, only the major results are summarized below.

Maturity of organic matter

The pyrolysis parameter T_{max} is intimately associated with the thermal history of OM (Tissot and Welte 1984). The

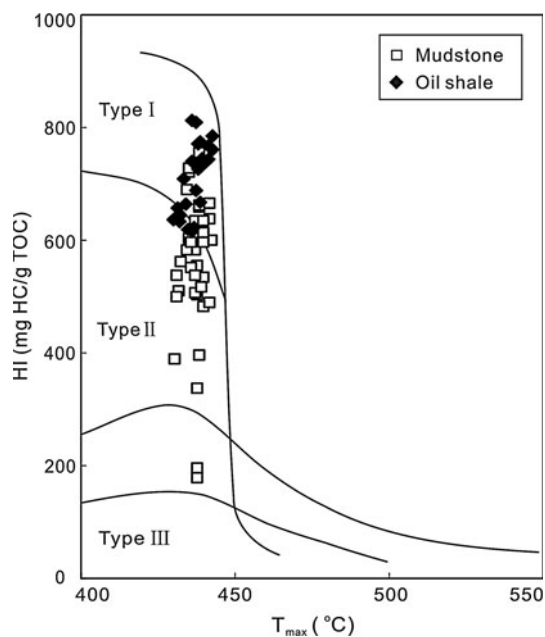


Fig. 5 Plot of T_{\max} versus HI (according to Espitalié et al. 1984)

low T_{\max} (430–440 °C) (Fig. 4f) values, together with the presence of type-I kerogen (Fig. 5), indicate the low maturity of OM in the oil shale sequences. The extractable organic matter (EOM or bitumen) yield varies between 37.1 and 57.2 mg/g TOC (Table 1), reflecting immaturity to marginal maturity of the oil shale samples (Tissot and Welte 1984; Peters and Moldowan 1993).

The 17β , $21\alpha(\text{H})\text{-C}_{30}$ hopane (moretane)/ 17α , $21\beta(\text{H})\text{-C}_{30}$ hopane ratios of the oil shales vary between 0.38 and 0.65, indicating immaturity of OM (Table 1). The $22\text{S}/(22\text{S} + 22\text{R})$ homohopane ratios can also be used to characterize the maturity of OM (Waples and Machihara 1991; Peters and Moldowan 1993). The equilibrium value for S/R isomerization of homohopanes is reached at 0.57–0.6 (Seifert and Moldowan 1986). The ratios obtained for all oil shale samples vary between 0.39 and 0.43 (Table 1), lower than the equilibrium value reflecting the low maturity of the oil shales.

Origin of OM input

The *n*-alkane distribution patterns of immature samples can be used to assess OM input from different producers (Fig. 6a; Brassell et al. 1978). Long-chain *n*-alkanes ($>n\text{-C}_{27}$) are characteristic biomarkers for higher terrestrial plants, whereas short-chain *n*-alkanes ($<n\text{-C}_{20}$) are found predominantly in algae and microorganisms. The *n*-alkanes of intermediate molecular weight ($n\text{-C}_{21-25}$) are reported to have originated from sphagnum or aquatic macrophytes (Bechtel et al. 2007). Higher relative proportions of short- to mid-chain *n*-alkanes (0.44) in comparison with long-chain

n-alkanes (0.38) are detected in the oil shale samples (Fig. 6a). Together with the fact that terrigenous OM is generally overestimated based on *n*-alkanes, since land plants typically contain more *n*-alkanes than aquatic OM (Peters et al. 2005), the results indicate a major contribution of aquatic organisms to OM deposition.

High contents of steroids and steroids/hopanoids ratios (≥ 1) indicate the predominance of OM production by phytoplankton (Moldowan et al. 1985). In contrast, lower contents of steroids and steroids/hopanoids ratios (< 1) suggest a high contribution of microbial biomass (Tissot and Welte 1984). In the present case, the high steroids/hopanoids ratios (Table 1) most probably reflect eutrophication and high bio-productivity within the photic zone of the water columns, and limited importance of cyanobacteria as primary producers (Peters et al. 2005).

Algae are the predominant primary producers of C_{27} sterols, while C_{29} sterols are more typically associated with land plants (Volkman 1986). In most oil shale samples, the C_{27} steranes predominate over the C_{29} and C_{28} steranes ($\text{C}_{27} > \text{C}_{29} > \text{C}_{28}$) (Table 1; Fig. 6c). The relative proportions of C_{27} , C_{28} , and C_{29} steranes in the ternary plot (Fig. 7) indicate a tendency towards higher proportions of C_{27} steranes in the oil shales than the mudstones. The sterane distribution patterns (Fig. 6c) are consistent with the dominant contribution of aquatic algae to OM production. However, numerous results from recent biomarker studies add to the growing list of microalgae that contain high proportions of 24-ethylcholesterol (Volkman et al. 1999).

Methylsteroids with a C_{30} dinosterol structure are considered as biomarkers of dinoflagellates (Robinson et al. 1984), while other C_{30} 4-methylsteroids appear to be related to marine and lacustrine precursors (Volkman et al. 1990; Peters et al. 2005). The 4-methylsteranes can be present in marine and lacustrine environments (Brassell et al. 1986; Summons et al. 1992; Peters et al. 2005). The high contents of 4-methylsteranes most probably originated from dinoflagellates. Abundant 4-methylsteroids (948 $\mu\text{g/g}$ TOC) are detected in all oil shale samples of the $\text{K}_{2\text{qn}1}$ (Table 1; Fig. 6d), indicating that some species of dinoflagellates adapted to living in the saline water environment at that time, as confirmed by research from Gao et al. (1992).

The outlined biomarker data argue for algae predominance in OM input. This interpretation is further supported by laminated algenites, accounting for up to 38 vol.% of macerals, and telalgenite (*botryococcus*), representing up to 6 vol.% of particulate OM (Fig. 8).

Terrigenous detrital matter input

The detrital input can be characterized by trace element analyses based on the principle of element migration and

Table 1 Concentration and concentration ratios of compounds and compound groups in hydrocarbon fractions of samples from the Qingshankou Formation

Sample	Depth (m)	C "BA" ^a (wt%)	EOM ^b (mg/g TOC)	Sum <i>n</i> -alkanes (μg/g TOC)	Pr ^d /Ph ^e	C _{27–29} steranes (μg/g TOC)	C ₂₇ /C ₂₉ steranes	4-Methyl-steranes (μg/g TOC)	C _{29–30} hopanes (μg/g TOC)
S 69	159.22	0.11	18.9	791	0.76	117	0.52	295	421
S 65	174.39	0.06	38.7	1,201	0.60	465	0.61	1,172	554
S 62	182.30	0.16	32.8	1,046	0.99	360	0.85	1,408	772
S 58	197.66	0.11	28.8	862	0.84	251	0.55	498	449
S 56	205.60	0.08	21.5	1,818	0.92	261	0.53	284	370
S 54	212.00	0.12	15.5	1,073	0.70	177	0.59	230	250
S 50	222.05	0.37	45.1	963	0.44	424	0.60	429	277
S 45	224.75	0.14	43.8	1,458	0.43	853	0.72	999	742
S 41	227.63	0.16	61.0	1,552	0.45	902	0.36	761	487
S 36	230.31	0.14	69.5	1,334	0.36	987	0.48	515	403
S 35	230.35	0.03	47.2	1,059	0.41	854	0.88	750	563
S 29	232.15	0.61	43.0	656	0.43	601	1.47	854	557
S 30	232.19	1.02	57.2	541	0.36	868	1.38	1,627	721
S 27	232.74	0.67	52.9	1,094	0.45	1,248	1.26	850	661
S 25	232.94	0.43	52.0	474	0.33	1,009	1.35	1,050	559
S 22	234.17	0.31	42.7	1,069	0.42	852	1.12	1,045	530
S 17	235.60	0.29	49.4	1,619	0.54	1,370	1.34	1,858	1,239
S 12	237.69	0.20	45.6	1,328	0.55	894	1.31	1,275	723
S 08	239.43	0.25	59.4	1,720	0.42	1,782	1.68	1,948	920
S 04	240.20	0.20	37.1	947	0.40	859	1.33	587	529
S 03	241.22	0.06	38.1	2,166	0.27	902	0.89	771	509
S 02	241.85	0.04	34.7	1,514	0.62	822	1.01	423	344
S 01	242.55	0.02	24.3	236	0.74	119	0.67	112	63
Average Oil shale		0.45	43.9	937	0.45	823	1.16	948	591
Mudstone		0.11	40.3	1,292	0.60	684	0.79	801	523

Sample	S/(S + R)	αβ-C ₃₁ hopanes	GI ^e	β-Carotene (μg/g TOC)	βα-Moretanes/αβ-hopanes	MTTC ^f ratio	C ₁₄ -aryl-isoprenoid (μg/g TOC)	Steroids/hopanoids
S 69	0.39		0.08	12.2	0.42	0.74	0.6	0.87
S 65	0.42		0.30	34.0	0.46	0.68	0.90	2.81
S 62	0.42		0.20	34.7	0.37	0.83	1.20	2.14
S 58	0.43		0.19	26.7	0.62	0.75	1.70	1.51
S 56	0.45		0.32	40.2	0.46	0.70	1.50	1.30
S 54	0.43		0.37	21.4	0.43	0.73	2.00	1.50
S 50	0.40		0.76	47.2	0.38	0.57	2.50	2.80
S 45	0.41		0.36	68.8	0.59	0.62	1.70	2.36

Table 1 continued

Sample	S/(S + R) $\alpha\beta$ -C ₃₁ hopanes	GI ^e	β -Carotene ($\mu\text{g/g}$ TOC)	$\beta\alpha$ -Moretanes/ $\alpha\beta$ -hopanes	MTTC ^f ratio	C ₁₄ -aryl-isoprenoid ($\mu\text{g/g}$ TOC)	Steroids/hopanoids
S 41	0.39	0.39	59.6	0.57	0.65	1.90	3.16
S 36	0.41	0.31	37.6	0.62	0.62	1.80	3.54
S 35	0.41	0.40	21.0	0.53	0.59	1.70	2.75
S 29	0.40	0.31	37.2	0.65	0.66	3.00	3.50
S 30	0.42	0.39	30.0	0.57	0.61	2.80	2.57
S 27	0.43	0.52	43.6	0.51	0.57	1.90	3.19
S 25	0.41	0.57	66.2	0.47	0.55	2.60	3.17
S 22	0.39	0.58	56.8	0.57	0.57	2.30	3.43
S 17	0.40	0.28	48.5	0.50	0.62	1.10	2.48
S 12	0.41	0.30	44.3	0.53	0.56	1.60	2.84
S 08	0.41	0.55	94.9	0.48	0.51	1.80	3.87
S 04	0.41	0.27	23.3	0.61	0.53	1.30	2.50
S 03	0.45	0.42	33.4	0.62	0.50	1.60	2.82
S 02	0.39	0.27	45.7	0.57	0.65	1.20	3.12
S 01	0.40	0.24	1.7	0.69	0.74	0.80	3.33
Average	0.41	0.45	41.6	0.52	0.60	2.20	2.79
	0.41	0.31	39.6	0.54	0.65	1.40	2.60

^a Chloroform bitumen "A"

^b Extractable organic matter

^c Pristane

^d Phytane

^e Gammacerane index = gammacerane/*n*-C₃₀ hopanoids ratio

^f 2-(4',8,12'-trimethyltridecyl) chroman

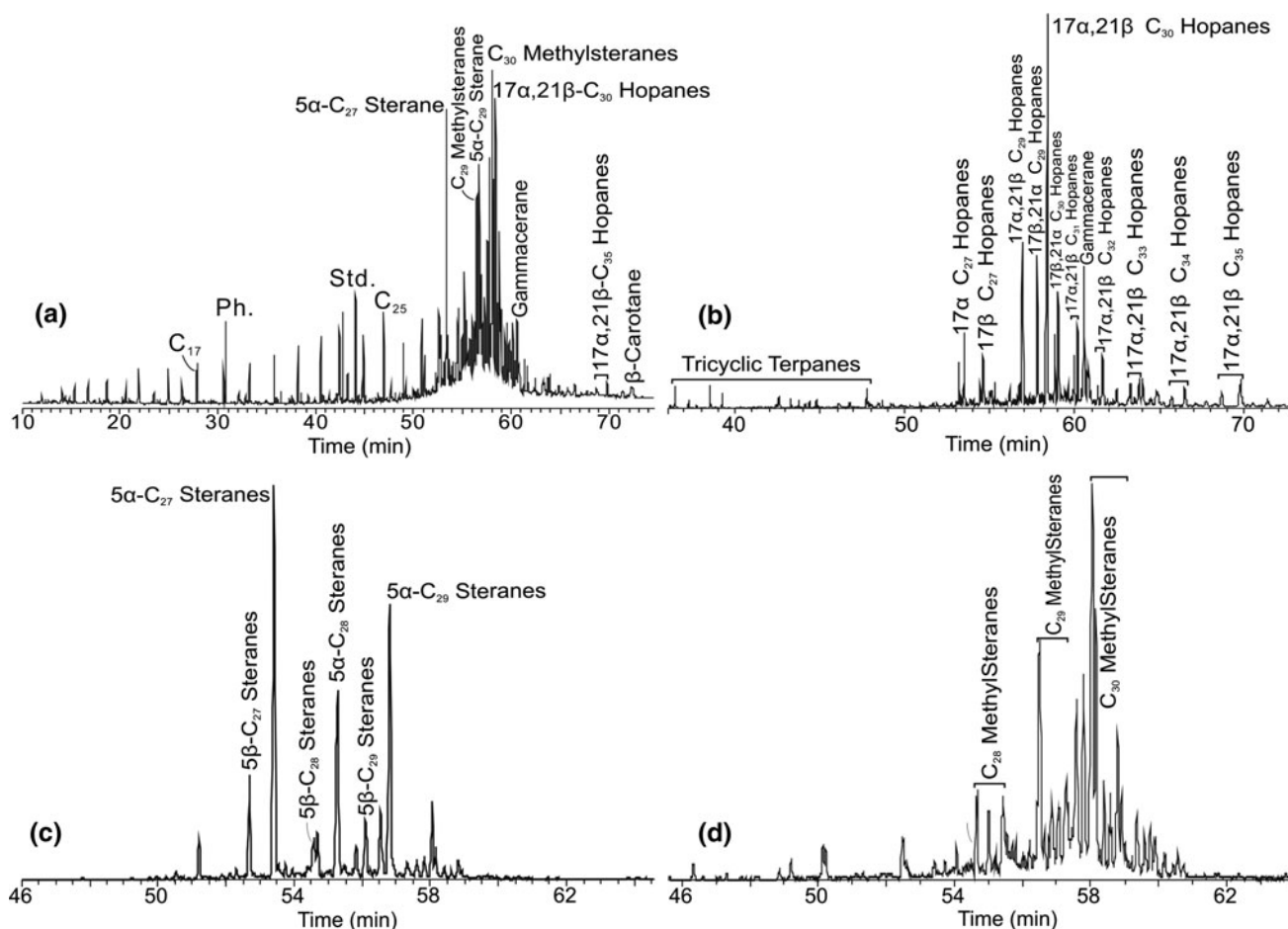


Fig. 6 Saturated hydrocarbon fractions for oil shale (sample S29) from the Qingshankou Formation. **a** Gas chromatograms (TIC), **b** m/z 191 for hopanes, **c** m/z 217 for steranes, and **d** m/z 231 for methylsteranes. *Ph.* phytane, *Std.* standard

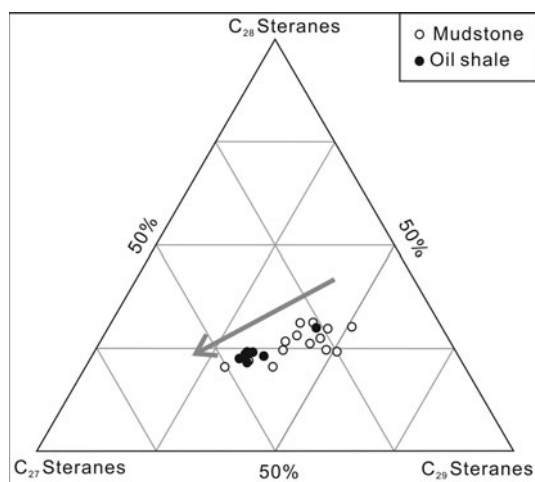


Fig. 7 Ternary plot of relative proportions of C_{27} , C_{28} , and C_{29} steranes for the Qingshankou Formation

sedimentary differentiation. Aluminium (Al) and titanium (Ti) are enriched mainly in the clay minerals, reflecting the input of detrital minerals (Deng and Qian 1993; Wang et al.

1997). In contrast to Al, Ti cannot be incorporated into siliceous deposits in neutral-to-alkaline environments. Therefore, Ti is used as an indicator of detrital matter input. In general, a higher content of Ti reflects an increased input of detrital matter.

Moderate contents of Ti (0.29 %) are detected in the lower oil shale sequence of the K_2qn_1 , and low contents of Ti (0.24 %) are present in the upper oil shale sequence, which are far less than those within the mudstone sequence (up to 0.39 %). The data indicate moderate detrital input during the deposition of the oil shales. Low input of mineral matter minimizes the effect of OM dilution.

Redox conditions

Vanadium (V) and nickel (Ni) are important indicators for the redox conditions. Vanadium is usually enriched in comparison with nickel in anoxic environments (Lewan and Maynard 1982; Peters and Moldowan 1993). In general, a high V/Ni ratio reflects a reducing environment, and a low ratio indicates oxic conditions. The higher V/Ni

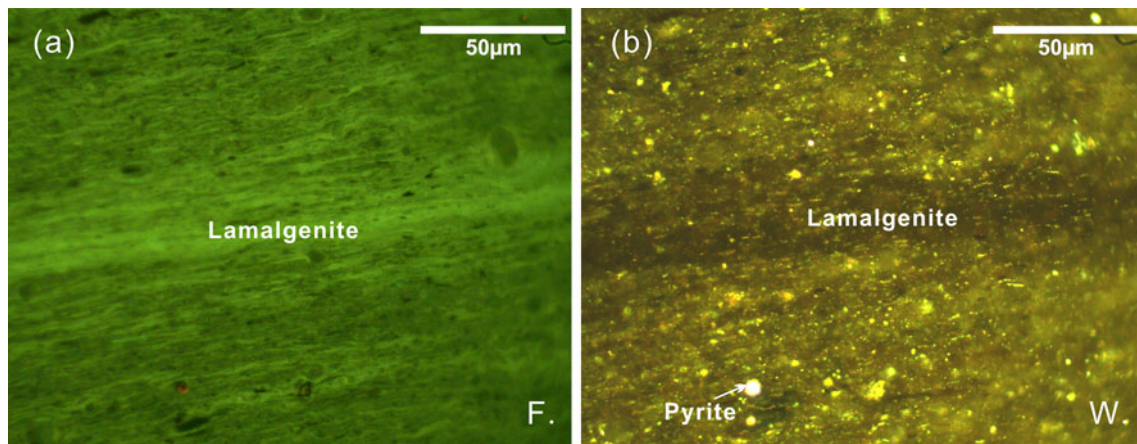


Fig. 8 Polished section under oil immersion from S29 of Well Ngn2. **a** Reflected fluorescence, **b** white light

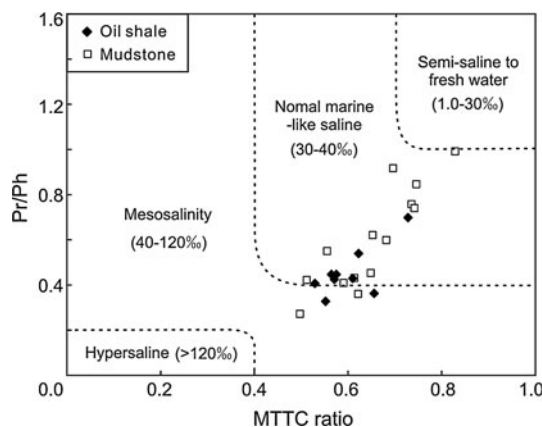


Fig. 9 Proposed revision of salinity inferences from MTTC ratio versus Pr/Ph for the Qingshankou Formation (after Schwark et al. 1998)

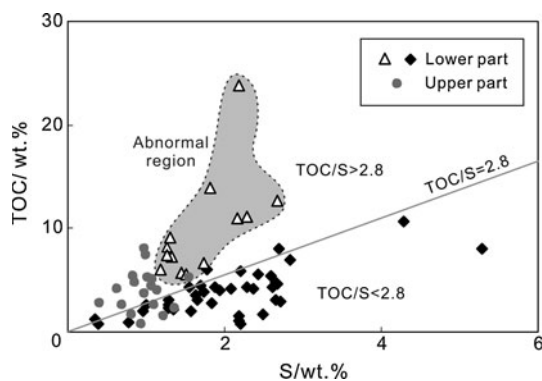


Fig. 10 Cross correlation between total sulphur (S) versus TOC for the Qingshankou Formation

ratios of the oil shales (4.6) relative to the mudstones (2.8) (Fig. 11) in the K₂qn₁ sediments are consistent with the proposed anoxic environment during the deposition of the oil shale sequences. This interpretation is confirmed by

Pr/Ph ratios significantly lower than 1.0 (Table 1), reflecting anoxic bottom water conditions (Didyk et al. 1978; Kohnen et al. 1991). The increased abundance of the C₃₅ homohopanes relative to the C₃₃ and C₃₄ homologues further indicates an anoxic environment during the deposition of the oil shale sequences (Peters and Moldowan 1993).

Aryl-isoprenoids are thought to derive from carotenoids specific for the photosynthetic green sulphur bacteria (Summons and Powell 1987). These organisms are phototrophic anaerobes and thus require both light and H₂S for growth. The C₁₄-arylisoprenoid present in the oil shale samples (2.2 µg/g TOC) (Table 1) is interpreted as an indicator for the activity of phototrophic anaerobes during periods of enhanced salinity stratification and euxinic conditions within the water column.

Lake water salinity

Strontium (Sr) and barium (Ba) are two elements with different geochemical behaviour in various sedimentary environments (Liu et al. 1984; Wang 1996). The Sr/Ba ratio is widely regarded as an empirical indicator of paleosalinity (Liu 1980). In general, a high Sr/Ba ratio reflects high salinity, and a low Sr/Ba ratio indicates low salinity (Deng and Qian 1993). The oil shale sequences show high Sr/Ba ratios (0.85), indicating a saline water environment during their deposition (Fig. 11). Abnormally, high Sr/Ba ratios (1.2; Fig. 11) are observed in a few samples of the lower oil shale sequence, which could be due to periodic sea water intrusion with high contents of strontium (up to 756 µg/g) during the early deposition of the K₂qn₁.

Gammacerane is a major biomarker in many lacustrine and marine sediments, indicating salinity stratification of the water columns during their deposition (Sinninghe Damsté et al. 1995; Grice et al. 1998). High gammacerane index values are often associated with low Pr/Ph ratios and

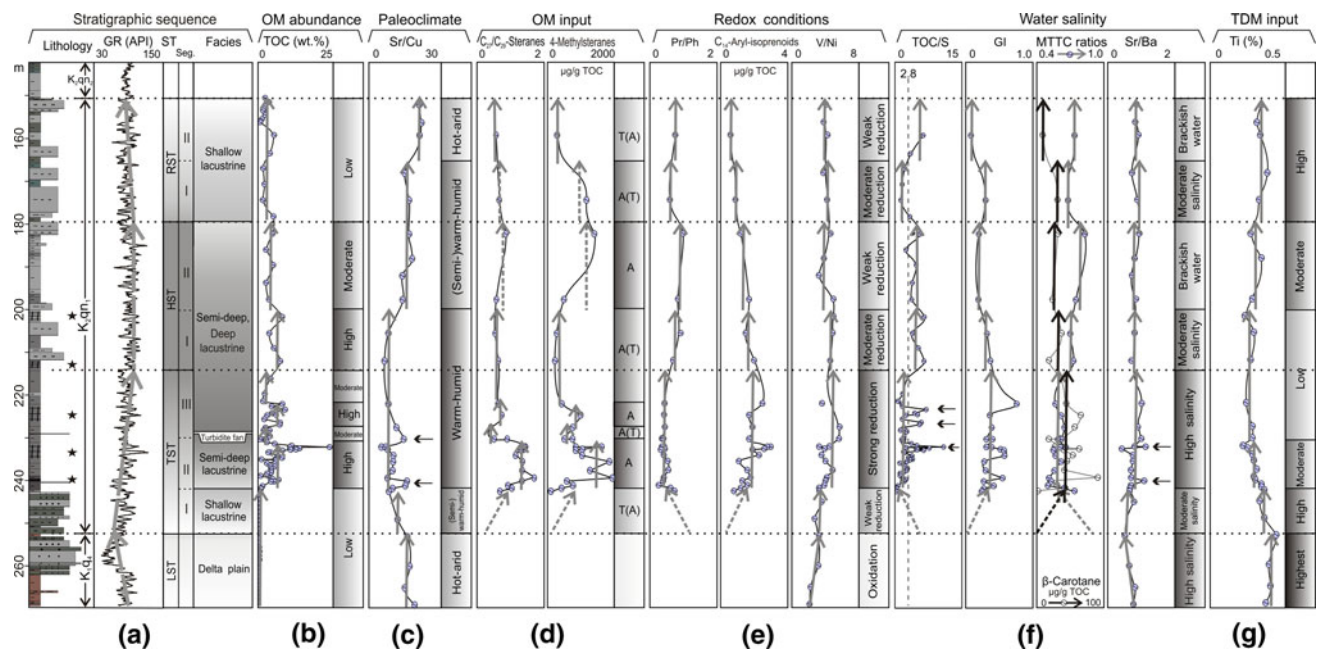


Fig. 11 The vertical evolution of OM enrichment in the different system tracts. *LST* lowstand systems tract, *TST* transgressive systems tract, *HST* highstand systems tract, *RST* regressive systems tract, *OM* organic matter, *TDM* terrigenous detrital matter, *A* aquatic organism,

T high plants, *ST* system tract, *Seg.* segment of organic matter in system tract. *Dotted arrows* inferred trend, *straight arrow* abnormal samples

the presence of carotenoids in the extracts (Peters et al. 2005). Abundant gammacerane contents with high gammacerane index (0.45) (Table 1) and moderate β -carotene contents (41.6 $\mu\text{g/g}$ TOC) (Table 1) are detected in all oil shale samples of the K_2q_{n1} , which provides evidence for water column stratification associated with increased salinity in the bottom waters during the deposition of the oil shale sequences.

Although the MTTC ratios are widely used as an indicator of paleosalinity, the reason for the correlation is unknown because the origin of MTTCs is unclear (Sinninghe Damsté et al. 1993; Barakat and Rullkötter 1997; Peters et al. 2005). By referring to the variation of Pr/Ph versus MTTC ratio and the salinity region division proposed by Schwark et al. (1998), differences in water column salinity are suggested. All samples are distributed within the regions of normal marine-like salinity and mesosaline conditions. A general tendency towards lower MTTC ratios with decreasing Pr/Ph ratios is observed (Fig. 9). This is in agreement with the interpretation of low Pr/Ph ratios of the oil shale sequences reflecting enhanced salinity stratification of the water column (ten Haven et al. 1988).

The ratio of TOC to total sulphur content (TOC/S) can be used as an indicator of lacustrine versus marine environments. Empirical investigations relate TOC/S values of about 2.8 ± 0.8 to marine conditions, whereas values $\gg 2.8$ may be indicative of freshwater conditions (Berner

and Raiswell 1983; Berner 1984). The TOC/S ratios within the lower part of oil shales (below 220 m) are almost all < 2.8 (Figs. 10, 11) with high S contents (Fig. 4b), indicating a high saline water environment. However, there are some samples below 220 m with higher TOC/S ratios (3.7–10.9) (Fig. 11) as a result of sulphate-limited pyrite formation during periods of high OM productivity and deposition (abnormal region in Fig. 10). Despite the higher concentration of sulphate in the saline water compared with fresh water, all soluble SO_4^{2-} ions were reduced by the high contents of OM, leading to high contents of residual OM with high TOC/S ratios (abnormal region in Fig. 10). In contrast, pyrite formation in the upper part (above 220 m) was limited by sulphate availability (~ 1.0 wt% S) (Fig. 4b) during periods of moderate to low OM productivity, as reflected by the lower average TOC values (Fig. 4a). Therefore, the high TOC/S ratios exceeding or near 2.8 in the upper part are interpreted as reflecting decreased water salinity (Fig. 11). This interpretation is confirmed by low gammacerane index, low β -carotene contents, and high MTTC ratios.

Paleoclimate reconstruction

The strontium (Sr)/copper (Cu) ratio is an important elemental indicator for paleoclimate reconstruction (Lerman 1989; Wang et al. 1997). In general, Sr/Cu ratios between 1.3 and 5.0 indicate a warm-humid climate, whereas a ratio

>5.0 points to a hot-arid climate (Lerman 1989). However, concentrations of Sr and Cu will be influenced by the scale of the lake basin, the offshore distance, and the water depth. However, high Sr/Cu ratios are suggested to reflect a hot-arid climate, and low Sr/Cu ratio indicates a warm-humid climate.

A Sr/Cu ratio of 10.0 was taken as the boundary for the climate division of the K_2qn_1 . The lower Sr/Cu ratios within the oil shale sequences (8.2) (Fig. 11) indicate a warm-humid climate, and the higher Sr/Cu ratios within the mudstone sequences (15.6) (Fig. 11) reflect a hot-arid climate. This interpretation is confirmed by new evidence from spore/pollen and oxygen isotope data (Wang et al. 2012). High Sr/Cu ratios (up to 15.2) (Fig. 11) found in some samples of the lower oil shale sequence may be caused by the periodic transgression events during the early K_2qn_1 .

Organic matter enrichment and sequence stratigraphy

Organic matter enrichment in the lacustrine sediments is controlled by the same factors as for other environments and can be expressed in a simple relation (Bohacs 1990, 1998; Bohacs et al. 2000):

$$\text{Organic Enrichment} = (\text{Production} - \text{Destruction})/\text{Dilution}$$

The above formula indicates that enrichment of OM should be enhanced during periods of high productivity, increased preservation of OM, and decreased dilution by mineral matter (Talbot 1988). The flourishing of aquatic organisms is beneficial to enhancement of biological productivity, anoxic bottom water conditions are favourable for OM preservation, and minor detrital matter input minimizes the dilution effect. However, moderate detrital matter input is associated with increased nutrient supply, promoting blooms of aquatic organisms.

According to the principle of continental sequence stratigraphy (Liu et al. 2002), a complete third-order sequence is recognized in the first Member of the Qingshankou Formation (K_2qn_1) and in the fourth Member of the Quantou Formation (K_1q_4) (Fig. 11a). The sequence is divided into four system tracts: lowstand system tract (LST), transgressive system tract (TST), highstand system tract (HST), and regressive system tract (RST). The enrichment of OM within the different system tracts of the K_2qn_1 was controlled by tectonics and climate, as outlined below.

1. The TST, during the period of lake-level rise (equivalent to the early period of the K_2qn_1), is marked by grey–green sands to dark-grey mudstones, developing from shallow to semi-deep to deep lacustrine facies (fining upward sequence; Fig. 11a). The climate gradually changed from hot-arid (LST) to warm-humid

(TST) (Fig. 11c) associated with a rapid tectonic subsidence, resulting in the rapid expansion of the lacustrine area. The rates of potential accommodation continuously exceeded water and sediment fill, indicating an under-filled stage (Carroll and Bohacs 1999). The transgression can be divided into three stages:

- I. The early (I) stage of TST is characterized by shallow lacustrine sediments (Fig. 11a) with low OM productivity [$100\text{--}200\text{ g}/(\text{m}^2\text{ a})$] (Ning et al. 2010). The OM derived from mixed sources of terrigenous plants and aquatic organisms (Fig. 11d). The V/Ni ratios (3.3) reflect a weakly reducing environment (Fig. 11e), confirmed by the Pr/Ph ratios (Feng et al. 2009b). The Sr/Ba ratios are approximately 0.6 (Fig. 11f; Wang et al. 1994), indicating a relatively low water salinity. Despite appropriate conditions for aquatic OM production and preservation, the high contents of the detrital mineral matter input (0.36 % Ti), as reflected by transgressive sand (Fig. 11a), led to low OM enrichment, due to dilution by the mineral matter.

- II. The middle (II) and late (III) stages of TST are characterized by (semi-)deep lacustrine deposition (Fig. 11a). The geochemical evidence, including low Pr/Ph ratios, high C_{14} -arylisoprenoid contents, and high V/Ni ratios (Fig. 11e), indicates a strongly reducing depositional environment with enhanced saline bottom water conditions, confirmed by low TOC/S ratios, high gammacerane index values, high β -carotene contents, low MTTC ratios, and high Sr/Ba ratios (Fig. 11f). During the stage of TST(II), high C_{27}/C_{29} sterane ratios (1.4) and abundant 4-methylsteranes (1,500 $\mu\text{g}/\text{g}$ TOC) (Fig. 11d) indicate the absolute predominance of aquatic organisms, with moderate detrital matter input (0.29 wt% Ti) (Fig. 11g), resulting in very high TOC contents (10.0 wt%) (Fig. 11b). However, during the stage of TST (III), moderate C_{27}/C_{29} sterane ratio (0.8) and decreased 4-methylsteranes contents (750 $\mu\text{g}/\text{g}$ TOC) (Fig. 11d) indicate the reduced contribution of aquatic organisms, causing the slightly lower TOC contents (4.0 wt%) (Fig. 11b).

2. The HST formed in a period of relatively stable lake-level (equivalent to the middle stage of the K_2qn_1), as marked by the deposition of the dark oil shales (Fig. 11a). The grey to dark-grey mudstones with grey muddy siltstones are characteristic for a (semi-)deep

lacustrine environment (Fig. 11a) with stable lake-level and shoreline. The potential accommodation approximately equals water and sediment fills (balanced-fill stage; Carroll and Bohacs 1999). The lake reached its maximum depth and extent with a stable salinity stratification of the water column. The HST can be divided into two stages:

- I. During the early (I) stage of HST, the low Sr/Cu ratios reflect a warm-humid climate (Fig. 11c). The moderate Pr/Ph ratios, C_{14} -arylisoprenoid contents, and V/Ni ratios (Fig. 11e) indicate a suboxic environment with moderate saline deep water conditions, confirmed by lower gammacerane index values, β -carotene contents, MTTC ratios, and Sr/Ba ratios (Fig. 11f). A mixed source with major contributions from aquatic organisms and minor inputs of land plants (Fig. 11d) as well as excellent OM preservation with low detrital matter input (Fig. 11g) led to a high TOC content (8.0 wt%) (Fig. 11b).
 - II. During the late (II) stage of HST, the climate changed into (semi-)warm-humid with higher Sr/Cu ratios (Fig. 11c). The increased C_{27}/C_{29} sterane ratios (0.7) and 4-methylsterane contents (1,000 $\mu\text{g/g}$ TOC) (Fig. 11d) indicate the predominance of aquatic organisms (green algae, dinoflagellates) in the OM production, deposited under weakly reducing conditions (Fig. 11e) within a brackish water environment (Fig. 11f). An enhanced detrital matter input is suggested by higher Ti contents (0.30 %) (Fig. 11g). The decreased TOC contents (5.0 wt%) (Fig. 11b) are probably caused by less favourable conditions for OM preservation.
3. The RST is defined by an initial drop of the lake-level (equivalent to the late period of the K_2qn_1), marked by the appearance of grey–green mudstones of shallow lacustrine facies (coarsening upward sequence; Fig. 11a). The climate gradually changed from (semi-)warm-humid to hot-arid (Fig. 11c) accompanied by slower tectonic subsidence, resulting in a smaller lacustrine area. The influx rate of water and sediment fill generally exceeded the available accommodation space (over-filled stage; Carroll and Bohacs 1999). The RST can be divided into two stages:
 - I. During the early (I) stage of RST, the geochemical data indicate moderately reducing bottom water conditions (Fig. 11e) and a moderately saline depositional environment (Fig. 11f). The predominance of aquatic organisms is confirmed by higher

C_{27}/C_{29} sterane ratios and 4-methylsterane contents (Fig. 11d), favoured by the (semi-)warm-humid climate (Fig. 11c). However, the OM enrichment (Fig. 11b) is diluted by the high mineral matter input (0.35 % Ti) (Fig. 11g).

- II. During the late (II) stage of RST, the lake shrunk and fluvial systems developed. A higher contribution of land plants to OM deposition (Fig. 11d) under weakly reducing conditions (Fig. 11e) and within a brackish water environment (Fig. 11f) is suggested by geochemical data. Moreover, the enhanced detrital matter input (Fig. 11g) under a hot-arid climate is confirmed by higher Ti contents (Fig. 11c). Therefore, this stage is characterized by low OM enrichment (Fig. 11b).

A model for changing environmental conditions leading to OM accumulation during different system tracts is presented (Fig. 12).

1. During the under-filled stage of the TST, the rapid tectonic subsidence and warm-humid climate resulted in the establishment of a deep lake. Salinity stratification with highly saline and strongly reducing bottom water was responsible for excellent OM preservation. Moreover, the flourishing of the aquatic organisms (dinoflagellates, green algae, *botryococcus*) was further promoted by moderate input of nutrients with weaker dilution effects, leading to high OM productivity. These conditions led to OM enrichment with high TOC content up to 23.0 wt% (Fig. 12a).
2. During the balanced-filled stage of the HST, the lake reached its maximum depth owing to sustained tectonic subsidence and warm-humid to (semi-)warm-humid climate. The enhanced freshwater input resulted in a decrease in water salinity, reducing the abundance of saline-tolerant organisms under the action of low input of nutrients. A lower OM productivity by freshwater algae is occurred. Therefore, OM enrichment decreased, as indicated by TOC contents of up to 8.0 wt% (Fig. 12b).
3. During the over-filled stage of the RST, the hot-arid climate caused a shrinking lake-level, indicated by the occurrence of shallow lacustrine sediments. Increased input of detrital matter and land plants lowered OM enrichment, and the TOC reached values up to 4.0 wt% (Fig. 12c).

The high water salinity during the early deposition of the Qingshankou Formation in the Songliao Basin could be caused by marine transgression events. Evidence comes mainly from the presence of marine organisms (bivalve) (Gu et al. 1976), fossil fish (Zhang and Zhou 1978), dinoflagellates (Gao et al. 1992), calcareous nannofossils

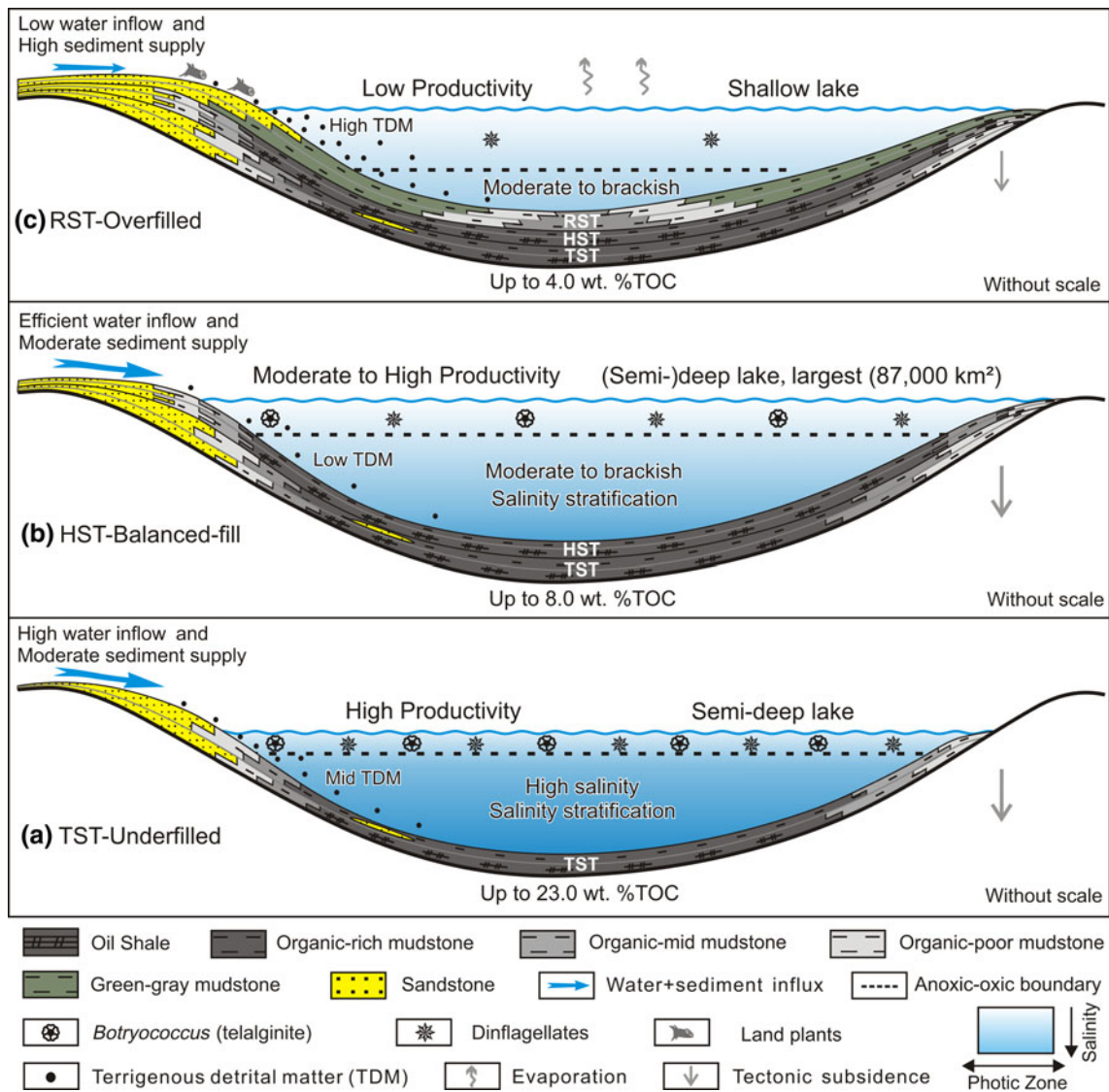


Fig. 12 The OM evolution model of the different system tracts in the Qingshankou Formation

(Ye and Wei 1996), foraminifera (Xi et al. 2011), marine biomarkers (dinosteranes, C₃₀ steranes) (Hou et al. 1999, 2000; Feng et al. 2009b), and authigenic glauconite (Chen 1980). However, the abundance and diversity of marine organisms in the Songliao Basin show great differences in comparison with the marine environment and biota (Huang et al. 1999b; Mao and Yu 1990; Sun et al. 1997). During the period of LST of the K_{1q4}, the development of evaporates under the hot-arid climate (Wang et al. 1995; Huang et al. 1999b) resulted in high salinity within the basin. With the development of TST of the K_{2qn1} under the humid-warm climate (Huang et al. 1999b) and the rapid tectonic subsidence (Feng et al. 2010), evaporates of older layers may have been dissolved, leading to salinity stratification of the water column. During the period of HST, the lake reached its maximum depth and extent (Huang et al.

1999b). The high input of freshwater decreased water salinity. During the period of RST, the lake-level dropped as a result of the hot-arid climate (Huang et al. 1999b) and slower tectonic subsidence.

Summary and conclusions

The development of the oil shale was controlled by warm-humid climate and tectonic subsidence in the K_{2qn1} of the Songliao Basin. In the oil shale sequences, high TOC content, potential yield, and chloroform bitumen “A” contents indicate high OM accumulation rates. The predominance of type-I kerogen and a low maturity of OM are evident. High relative proportions of short- to mid-chain *n*-alkanes in comparison with long-chain *n*-alkanes, high steroid/hopanoid ratios, the

predominance of $C_{27} + C_{28}$ over C_{29} regular steranes, abundant 4-methylsteroids, and algal-derived macerals [lamalgenite (38 vol.%) and telalgenite (*botryococcus*) (6 vol.%)] provide evidence for the predominance of aquatic phytoplankton. Moderate input of detrital matter and persistent nutrient supply promoted blooms of aquatic organisms. The presence of reducing saline bottom water conditions and minor dilution effects by mineral matter, indicated by geochemical parameters, led to excellent preservation of OM.

The K_{29n1} of the Songliao Basin represents a third-order sequence divided into three system tracts (TST, HST, RST), which can be related to differences in OM accumulation rates. The inputs of OM changed from the terrigenous-derived OM stage (TST-I) to the blooms of aquatic organisms (TST-II). Decreasing contributions of aquatic organisms (TST-III–HST-I) were followed by intensified autochthonous OM production during HST-II–RST-I. During RST-II, intensified OM input from land plants occurred. The redox conditions of the lake changed from the weakly reducing (TST-I) to anoxic (TST-II and -III), followed by a decrease in bottom water reductivity (HST-I and -II). Finally, increasing Eh is occurred during stages RST-I and RST-II. Salinity within the lake changed from mesosaline (TST-I, -II and -III) to normal marine-like salinity (stage of HST-I and -II). Salinity in the bottom water decreased during stages RST-I and RST-II. The detrital matter input was higher during TST-I than during stages TST-II/III and HST-I/II, followed by enhanced input during RST-I and RST-II. The outlined changes in the paleoenvironment are related to differences in OM accumulation rates, which changed from low values (TST-I) to high-moderate values during stages of TST-II/III and HST-I/II, and finally to low values during RST-I and RST-II.

High OM enrichment is found in the stages of mid-late TST and early HST. Under the control of warm-humid climate and tectonic subsidence during these stages, the (semi-) deep lacustrine environment provided the location for the blooms of aquatic organisms. Moderate detrital input delivered nutrients enhancing OM productivity. Salinity stratification of the water column and reducing bottom water conditions was favourable for OM preservation.

Acknowledgments Measurement of samples and discussion with Dr. R. Gratzner, Dr. D. Reischenbacher, and Dr. J. Gusterhuber during the laboratory work are gratefully acknowledged. We thank Prof. Dr. R. F. Sachsenhofer for his helpful discussion and suggestions. This paper benefited greatly from the critical comments of two anonymous reviewers and the topic editor of the *International Journal of Earth Sciences*. The research project was supported financially by the Basic Outlay of Scientific Research Work from the Ministry of Science and Technology of China (No. J1220), and the National Natural Science Foundation of China (No. 40972076). All the organic geochemical data were measured at the Department of Applied Geosciences and Geophysics at the Montanuniversität Leoben (Austria). Jianliang Jia also thanks the Austrian Exchange Service (OAD) for a 6-months' scholarship.

References

- Barakat AO, Rullkötter J (1997) A comparative study of molecular paleosalinity indicators: chromans, tocopherols and C_{20} isoprenoid thiophenes in Miocene lake sediments (Nördlinger Ries, Southern Germany). *Aquat Geochem* 3:169–190
- Bechtel A, Reischenbacher D, Sachsenhofer RF, Gratzner R, Lücke A, Püttmann W (2007) Relations of petrographical and geochemical parameters in the middle Miocene Lavanttal lignite (Austria). *Int J Coal Geol* 70:325–349
- Bechtel A, Jia JL, Strobl SAI, Sachsenhofer RF, Liu ZJ, Gratzner R, Püttmann W (2012) Paleoenvironmental conditions during deposition of the Upper Cretaceous oil shale sequences in the Songliao Basin (NE China): implications from geochemical analyses. *Org Geochem* 46:76–95
- Berner RA (1984) Sedimentary pyrite formation: an update. *Geochim Cosmochim Acta* 48:605–615
- Berner RA, Raiswell R (1983) Burial of organic carbon and pyrite sulfur in sediments over Phanerozoic time: a new theory. *Geochim Cosmochim Acta* 47:862–885
- Bohacs KM (1990) Sequence stratigraphy of the Monterey Formation, Santa Barbara County: integration of physical, chemical, and biofacies data from outcrop and subsurface. *SEPM Core Workshop* 14:139–201
- Bohacs KM (1998) Contrasting expressions of depositional sequences in mudrocks from marine to nonmarine environments. *Mudstones Shales* 1:32–77
- Bohacs KM, Carroll AR, Neal JE, Mankiewicz PJ (2000) Lake-basin type, source potential, and hydrocarbon character; an integrated sequence-stratigraphic-geochemical framework (in lake basins through space and time). *AAPG Stud Geol* 46:3–34
- Brassell SC, Eglinton C, Maxwell JR, Philp RP (1978) Natural background of alkanes in the aquatic environment. Pergamon Press, Oxford, pp 69–86
- Brassell SC, Eglinton G, Fu JM (1986) Biological marker compounds as indicators of the depositional history of the Maoming oil shale. *Adv Org Geochem* 10(4–6):927–941
- Carroll AR, Bohacs KM (1999) Stratigraphic classification of ancient lakes: balancing tectonic and climatic controls. *Geology* 27:99–102
- Carroll AR, Bohacs KM (2001) Lake-type controls on petroleum source rock potential in nonmarine basins. *AAPG Bull* 85:1033–1053
- Chen RJ (1980) Characteristics of glauconites from some regions and their significance in analyzing the facies environment. *Sci Geol Sin* 1:65–74 (in Chinese with English abstract)
- Chi XY (2010) Characteristics and sedimentary environment of oil shale in the Upper Cretaceous of Songliao Basin. *J Oil Gas Technol* 32:161–165 (in Chinese with English abstract)
- Deng HW, Qian K (1993) Analysis on sedimentary geochemistry and environment. Science Technology Press, Gansu, pp 15–85 (in Chinese)
- Didyk BM, Simoneit BRT, Brassell SC (1978) Organic geochemical indicators of paleo-environmental conditions of sedimentation. *Nature* 272:216–222
- Espitalié J, Marquis F, Barsony I (1984) Geochemical logging. In: Voorhess KJ (ed) *Analytical pyrolysis*. Butterworths, Boston, pp 53–79
- Feng ZH, Fang W, Zhang JH, Li ZG, Huang CY, Wang X, Zhao QL, Huo QL (2007) Distribution and significance of C_{40}^+ alkanes in the extracts of Cretaceous source rocks from the Songliao Basin. *Sci China Ser D Earth Sci* 50:1510–1520
- Feng ZH, Fang W, Wang X, Huang CY, Huo QL, Zhang JH, Huang QH, Zhang L (2009a) Microfossils and molecular records in oil shales of the Songliao Basin and implications for paleo-

- depositional environment. *Sci China Ser D Earth Sci* 52:1559–1571
- Feng ZH, Huo QL, Wang X, Fang W, Song ZG (2009b) Geochemical research on the Late Cretaceous strata of Well SK1 in Songliao Basin. *Earth Sci Front* 16:181–191 (in Chinese with English abstract)
- Feng ZQ, Jia CZ, Xie XN, Zhang S, Feng ZH, Timothy AC (2010) Tectonostratigraphic units and stratigraphic sequences of the nonmarine Songliao basin, northeast China. *Basin Res* 22:79–95
- Feng ZH, Fang W, Li ZG, Wang X, Huo QL, Huang CY, Zhao JH, Zeng HS (2011) Depositional environment of terrestrial petroleum source rocks and geochemical indicators in the Songliao Basin. *Sci China Ser D Earth Sci* 54:1304–1317
- Gao RQ, Cai XY (1997) Field formation conditions and distribution rules in Songliao Basin. *Petroleum Industry Press, Beijing*, pp 65–163 (in Chinese)
- Gao RQ, He CQ, Qiao XY (1992) A new genus and species of Cretaceous dinoflagellates from two transgressive beds in Songliao Basin, NE China. *Acta Palaeontol Sin* 31:17–29 (in Chinese with English abstract)
- Grice K, Schouten S, Peters KE, Sinninghe Damsté JS (1998) Molecular isotopic characterisation of hydrocarbon biomarkers in Palaeocene-Eocene evaporitic, lacustrine source rocks from the Jiangnan Basin, China. *Org Geochem* 29:1745–1764
- Gu ZW, Huang BY, Chen CZ (1976) Lamellibranchiata fossils of China. *Science Press, Beijing*, pp 80–110 (in Chinese)
- He JL, Deng SW, Chen WL, Jia YK, Gao JQ (2006) Evaluation of oil shale in the Southern Songliao Basin using logging techniques. *J Jilin Univ (Earth Sci Ed)* 36:909–914 (in Chinese with English abstract)
- Hou DJ, Huang QH, Huang FT, Kong QY (1999) The characteristics of molecular geochemistry of marine transgression strata in Songliao Basin. *Acta Petrol Sin* 20:30–34 (in Chinese with English abstract)
- Hou DJ, Li MW, Huang QH (2000) Marine transgressional events in the gigantic freshwater lake Songliao: paleontological and geochemical evidence. *Org Geochem* 31:763–768
- Huang FT, Chi YL, Huang QH (1999a) Doubts about the validity of the Middle Cretaceous transgression in Songliao Basin. *Petrol Explor Dev* 26:104–107 (in Chinese with English abstract)
- Huang QH, Zheng YL, Yang MJ, Li XJ, Han MX, Chen CR (1999b) On Cretaceous paleoclimate in the Songliao Basin. *Acta Micropalaeontol Sin* 16:95–103 (in Chinese with English abstract)
- Jia JL, Liu ZJ, Guo W, Liu R, Meng QT, Yan L (2011) Application of geological analogy to assess oil shale resources of depression basin—An example from Upper Cretaceous Songliao Basin. *J China Coal Soc* 36:1474–1480 (in Chinese with English abstract)
- Jia JL, Liu ZJ, Meng QT, Liu R, Sun PC, Chen YC (2012) Quantitative evaluation of oil shale based on well log and 3-D seismic technique in the Songliao Basin, Northeast China. *Oil Shale* 29:128–150
- Jia JL, Bechtel A, Liu ZJ, Strobl SAI, Sun PC, Sachsenhofer RF (2013) Oil shale formation in the Upper Cretaceous Nenjiang Formation of the Songliao Basin (NE China): implications from organic and inorganic geochemical analyses. *Int J Coal Geol* 113:11–26
- Kohnen MEL, Sinninghe Damsté JS, de Leeuw JW (1991) Biases from natural sulphurization in paleoenvironmental reconstruction based on hydrocarbon biomarker distribution. *Nature* 349:775–778
- Lerman A (1989) Lakes chemistry and geology physics. *Geological Press, Beijing*, pp 10–100 (in Chinese)
- Lewan MD, Maynard JB (1982) Factors controlling enrichment of vanadium and nickel in the bitumen of organic sedimentary rocks. *Geochim Cosmochim Acta* 46:2541–2560
- Liu BJ (1980) Sedimentary petrology. *Geological Press, Beijing*, pp 13–89 (in Chinese)
- Liu ZJ, Liu R (2005) Oil shale resource state and evaluating system. *Earth Sci Front* 12:315–323 (in Chinese with English abstract)
- Liu YJ, Cao LM, Li ZL, Wang HN, Chu TQ, Zhang JR (1984) Element geochemistry. *Science Press, Beijing*, pp 283–372 (in Chinese)
- Liu ZJ, Wang DP, Liu L, Liu WZ, Wang PJ, Du XD, Yang G (1993) Sedimentary characteristics of the cretaceous in the Songliao Basin. *Acta Geol Sin Engl Ed* 6:167–180
- Liu ZJ, Dong QS, Wang SM, Zhu JW, Guo W (2002) Introduction to continental sequence stratigraphy and application. *Petroleum Industry Press, Beijing*, pp 21–70 (in Chinese with English abstract)
- Liu ZJ, Yang HL, Dong QS, Zhu JW, Guo W, Ye SQ, Liu R, Meng QT, Zhang HL, Gan SC (2009) Oil shale in China. *Petroleum Industry Press, Beijing*, pp 157–189 (in Chinese with English abstract)
- Liu RH, Tang SH, Liang F (2010) Study on formation laws and controlling factors of oil shale deposits in extensional basins in Northeast China. *China Petrol Explor* 6:76–80 (in Chinese with English abstract)
- Mao SZ, Yu JX (1990) Origin and evolution of terrestrial dinoflagellates and their significance in source potential for petroleum. *Earth Sci J China Univ Geosci* 15:283–290 (in Chinese with English abstract)
- Moldowan JM, Seifert WK, Gallegos EJ (1985) Relationship between petroleum composition and depositional environment of petroleum source rocks. *AAPG Bull* 69:1255–1268
- Ning WK, Fu L, Huo QL (2010) Productivity of paleo-Songliao Lake during the Late Cretaceous in well Songke-1, Songliao Basin. *J Jilin Univ (Earth Sci Ed)* 40:1020–1034 (in Chinese with English abstract)
- Peters KE (1986) Guidelines for evaluating petroleum source rock using programmed pyrolysis. *AAPG Bull* 70:318–329
- Peters KE, Moldowan JM (1993) The biomarker guide: interpreting molecular fossils in petroleum and ancient sediments. *Prentice Hall, Englewood Cliffs*, pp 550–590
- Peters KE, Walters CC, Moldowan JM (2005) The biomarker guide, biomarkers and isotopes in petroleum exploration and earth history, vols 1 and 2. *Cambridge University Press, New York*
- Qu H, Hu SY, Meng QT (2006) Resource potential and policy proposes of oil shale in Songliao and Adjacent Basin. *J Jilin Univ (Earth Sci Ed)* 36:944–948 (in Chinese with English abstract)
- Radke M, Willsch H, Welte DH (1980) Preparative hydrocarbon group type determination by automated medium pressure liquid chromatography. *Anal Chem* 52:406–411
- Robinson N, Eglinton G, Brassell SC, Cranwell PA (1984) Dinoflagellate origin for sedimentary 4-methylsteroids and 5 (H)-stanols. *Nature* 308:439–442
- Schwark L, Vliex M, Schaeffer P (1998) Geochemical characterization of Malm Zeta laminated carbonates from the Franconian Alb, SW-Germany (II). *Org Geochem* 29:1921–1952
- Seifert WK, Moldowan JM (1986) Use of biological markers in petroleum exploration. *Methods Geochem Geophys* 24:261–290
- Sinninghe Damsté JS, Keely BJ, Betts SE, Baas M, Maxwell JR, de Leeuw JW (1993) Variations in abundances and distributions of isoprenoid chromans and long-chain alkylbenzenes in sediments of the Mulhouse Basin: a molecular sedimentary record of palaeosalinity. *Org Geochem* 20:1201–1215
- Sinninghe Damsté JS, van Duin ACT, Hollander D, Kohnen ML, de Leeuw JW (1995) Early diagenesis of bacteriohopanepolyol derivatives: formation of fossil homohopanoids. *Geochim Cosmochim Acta* 59:5141–5147
- Summons RE, Powell TG (1987) Identification of aryl isoprenoids in source rocks and crude oils: biological markers for the green sulphur bacteria. *Geochim Cosmochim Acta* 51:557–566

- Summons RE, Thomas J, Maxwell JR, Boreham CJ (1992) Secular and environmental constraints on the occurrence of dinosterane in sediments. *Geochim Cosmochim Acta* 56:2437–2444
- Sun ZC, Feng XJ, Yang P, Xu JL, Yang P, Li DM (1997) Discovery of Neogene–Quaternary foraminifera and calcareous nannofossils from western China and its geological significance. *Geoscience* 11:269–274 (in Chinese with English abstract)
- Talbot MR (1988) The origins of lacustrine oil source rocks: evidence from the lakes of tropical Africa. *Geol Soc Lond Spec Publ* 40:29–43
- ten Haven HL, de Leeuw JW, Sinninghe Damsté JS, Schenck PA, Palmer SE, Zumberge JE (1988) Application of biological markers in the recognition of palaeohypersaline environments. In: Kelts K, Fleet AJ, Talbot M (eds) *Lacustrine petroleum source rocks*. Geological Society special publication no. 26, Blackwell, Oxford, pp 123–140
- Tissot BP, Welte DH (1984) *Petroleum formation and occurrence*. Springer, New York, pp 600–705
- Volkman JK (1986) A review of sterol markers for marine and terrigenous organic matter. *Org Geochem* 9:83–99
- Volkman JK, Kearney P, Jeffrey SW (1990) A new source of 4-methyl steroids and 5 α (H)-stanols in sediments: prymnesiophyte microalgae of the genus *Pavlova*. *Org Geochem* 15:489–497
- Volkman JK, Barrett SM, Blackburn SI (1999) Eustigmatophyte microalgae are potential sources of C₂₉ sterols, C₂₂–C₂₈ *n*-alcohols and C₂₈–C₃₂ *n*-alkyl diols in freshwater environments. *Org Geochem* 30:307–318
- Wang AH (1996) Discriminant effect of sedimentary environment by the Sr/Ba ratio of different existing forms. *Acta Sedimentol Sin* 14:168–173 (in Chinese with English abstract)
- Wang YL (2006) Characteristics and depositional regularities of oil shale in Upper Cretaceous of southern Songliao Basin. Master's dissertation, Jilin University, pp 23–68 (in Chinese)
- Wang DP, Liu ZJ, Liu L (1994) The evolution and global eustasy of the Songliao Basin. *Geology Press, Beijing*, pp 54–89 (in Chinese)
- Wang PJ, Ren YG, Wang DP (1995) Evaporite origin and its palaeoenvironmental significance of Quantou Formation, Songliao Cretaceous Nearshore Continental Basin (NE China). *Acta Sedimentol Sin* 13:53–61 (in Chinese with English abstract)
- Wang PJ, Du XD, Wang J, Wang DP (1996) Chronostratigraphy and stratigraphic classification of the Cretaceous of the Songliao Basin. *Acta Geol Sin (Engl Ed)* 9:207–217
- Wang JS, Huang XZ, Sui JC, Shao HS, Yan CF, Wang SQ, He ZR (1997) Evolutional characteristics and their paleoclimate significance of trace elements in the Hetaoyuan Formation, Biyang depression. *Acta Sedimentol Sin* 15:65–70 (in Chinese with English abstract)
- Wang CS, Feng ZQ, Zhang LM, Huang YJ, Cao K, Wang PJ, Zhao B (2012) Cretaceous paleogeography and paleoclimate and the setting of SKI borehole sites in Songliao Basin, northeast China. *Palaeogeogr Palaeoclimatol Palaeoecol*. doi:10.1016/j.palaeo.2012.01.030
- Waples DW, Machihara T (1991) Biomarkers for geologists: a practical guide to the application of steranes and triterpanes in petroleum geology. AAPG methods in exploration series no. 9. Tulsa, Oklahoma, p 91
- Xi DP, Wan XQ, Feng ZQ, Li S, Feng ZH, Jia JZ, Jing X, Si WM (2011) Discovery of Late Cretaceous foraminifera in the Songliao Basin: evidence from SK-1 and implications for identifying seawater incursions. *Chin Sci Bull* 55:3433–3436 (in Chinese with English abstract)
- Ye SF, Wei KS (1996) Condensed section and new evidence of marine inundation in Cretaceous, Songliao Basin. *Earth Sci J China Univ Geosci* 21:267–271 (in Chinese with English abstract)
- Zhang MM, Zhou JJ (1978) On the fossil fishes in Mesozoic and Cenozoic oil-bearing strata from east China and their sedimentary environment. *Vertebrata Palasiatica* 16:229–237 (in Chinese with English abstract)